INTERATOM RESULTS FOR STAGE 2

D. COORS
Interatom GmbH,
Bergisch Gladbach,
Federal Republic of Germany

Abstract

This report contains the Interatom results for Stage 2 of the "IWGFR Program on Intercomparison of LMFBR Core Mechanics Codes" which was agreed upon on a Consultants Meeting in Vienna, 8-10 December, 1987 [1].

The calculations were performed with the 3D core mechanics code system DDT developed at Interatom and with the 2D core mechanics code FIAT.

---

1 Introduction

This report contains the Interatom results for the "IWGFR Programme on Intercomparison of LMFBR Core Mechanics Codes" which was agreed upon on a Consultants Meeting for the Coordinated Research Programme (CRP) in Vienna, 8 - 10 December 1987 [1].

The description of the three examples to be solved by the participants as defined in [1] is given in the Enclosure of this report.

2 Core Mechanics Codes

The results presented in this report are calculated with the 3d core mechanics code DDT [2, 3] which is the basic code of the DDT-system developed at Interatcm and with the 2d code FIAT [4].

The DDT code system consists of the following moduls:

- DDT: Thermal bow modul of the system. Calculation of hot geometry, free temperature bow of subassemblies, core mechanical equilibrium data for different levels of power to flow ratios and graphical display of results for core cross-sections.
- DDTR: Replaces DDT for calculations with friction.
- DDAB: Burnup modul of the system for consideration of swelling and creep.

DDT is applied for examples 1 and 2. DDTR and DDAB are not applied for the calculations presented in this report.

The FIAT-code combines the capabilities of DDT and DDAB in one code but on a 2d geometry basis. FIAT is applied for Example 3.

3 Preparation of Input

An extract of the experimental data which are presented in [5] and which are needed as input for DDT is attached as Enclosure to this report.

For a better judgement of the DDT results it is worthwhile to mention some properties of the DDT code concerning the treatment of the corresponding prescribed data.

All temperatures are assumed to be wrapper tube outwall temperatures. The azimuthal temperature profile is approached by six temperatures on the circumference of the wrapper tube each of them for the mid of one face. For the integration of the temperature profile a linear variation between these midface values is assumed. The temperatures for the corners are not considered. In Fig. 3.3 to 3.5 of the Enclosure both azimuthal profiles are compared, the measured one and the applied one. The resulting error for the free temperature bow of a subassembly due to the different profiles is assumed to be small.

The input of the geometric data is required for a temperature of 20 °C. The corresponding hot dimensions in radial and axial direction are internally calculated for the actual temperatures of the concerned axial nodes. These temperatures on their part are arithmetic mean values of the corresponding six midface temperatures which are the input values for the calculation of the thermal deflection of the subassemblies.

The different geometries of the spike cannot yet be modelled with DDT. So, for the spike the wrapper tube geometry has to be applied. The axial development of the moment of inertia for Examples 1A and 1B is shown in Figure 2 of Appendix 1 of the Enclosure. Simple considerations with the code FIAT with axial constant geometry and axial variable geometry show negligible differences of the results for both assumptions. This is also expected for Example 2 where the moments of inertia of some sub-assemblies differ somewhat from those of Examples 1A and 1B.

4 Results

4.1 Example 1B

- Free thermal bow of a single subassembly

The results for Example 1B are presented in Table 1 and in Figure 1. It can be seen that the agreement between the reference results and the measured values is good in the axial range of 0 to 1570 mm while it becomes worse above this region.

In order to fit the calculated curve to one of the measured data of the upper region the temperature gradient is adapted stepwise with 3 factors. They affect the gradients of all axial nodes with the same percentage.

Table 1: EXAMPLE 1B

Free temperature bow [mm] of a single sub-assembly for different temperature gradients.

Axial Position [mm]	Experiment	DDT-Results			
		Ref.	Ref. +9.7 %	Ref. +18.3 %	Ref. +27 %
570	0	0	0	0	0
770	0.2	0.5	0.05	0.05	0.06
970	0.4	0.35	0.38	0.41	0.44
1170	1.0	0.99	1.09	1.18	1.26
1370	1.6	1.98	2.17	2.34	2.52
1570	3.2	3.29	3.60	3.89	4.18
1770	5.4	4.92	5.39	5.82	6.25
1970	7.2	6.90	7.56	8.16	8.76
2170	10.8	9.14	10.01	10.81	11.60
2370	13.5	11.49	12.60	13.60	14.60

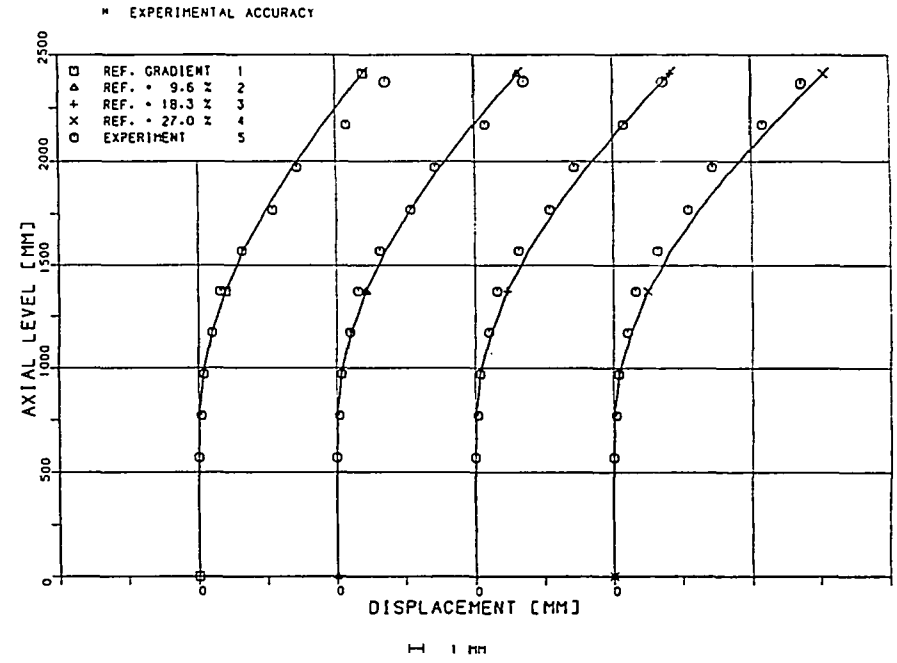

IWGFR STAGE 2 DDT EXAMPLE 1B
FREE TEMPERATURE BOW
VARIATION OF TEMP. GRADIENT

FIG. 1

4.2 Example 1A

- Restraint bow of a single subassembly

The results for Example 1A are presented in Table 2, 3 and Figures 2 and 3. It is obvious that there is no good agreement between measured and calculated reference values concerning deflections and loads as well.

Increasing the temperature gradient by 27 % (Figure 2) as in Example 1A and reducing additionally the pad stiffness to 1/3 (Figure 3) as proposed in [5] does not improve the agreement. In the upper part of the curve it becomes slightly better while it becomes worse in the lower part. Especially the maximum calculated deflection of -1.39 mm still differs distinctly from the measured value of -1.70 mm.

Table 2: EXAMPLE 1A

Restraint deflection [mm] of a single sub-assembly for different temperature gradients and different pad stiffnesses in LRP.

Axial Position [mm]	Experiment	DDT-Results		
		Reference	Temp.-Bow +27 %,	Temp.-Bow +27 %, lower pad stiffness -67 %
570	0	-0.58	-0.48	-0.71
770	-0.5	-0.84	-0.80	-1.04
970	-1.0	-1.03	-1.03	-1.29
1170	-1.70	-1.09	-1.14	-1.39
1370	-1.70	-1.04	-1.13	-1.36
1570	-1.50	-0.88	-1.00	-1.20
1770	-1.0	-0.60	-0.72	-0.89
1970	-0.6	-0.15	-0.26	-0.38
2170	0.3	0.43	0.36	0.30
2370	1.2	1.07	1.06	1.05

Table 3: EXAMPLE 1A

Forces [N] in contact levels for different temperature gradients and different lower pad stiffnesses

Axial Position [mm]	Experiment	DDT-Results		
		Reference	Temp.-Bow +27 %,	Temp.-Bow +27 %, lower pad stiffness -67 %
Spike bottom	not measured	94	142	129
Spike top	not measured	0	0	0
LRP	443	222	337	306
URP	211	128	195	177

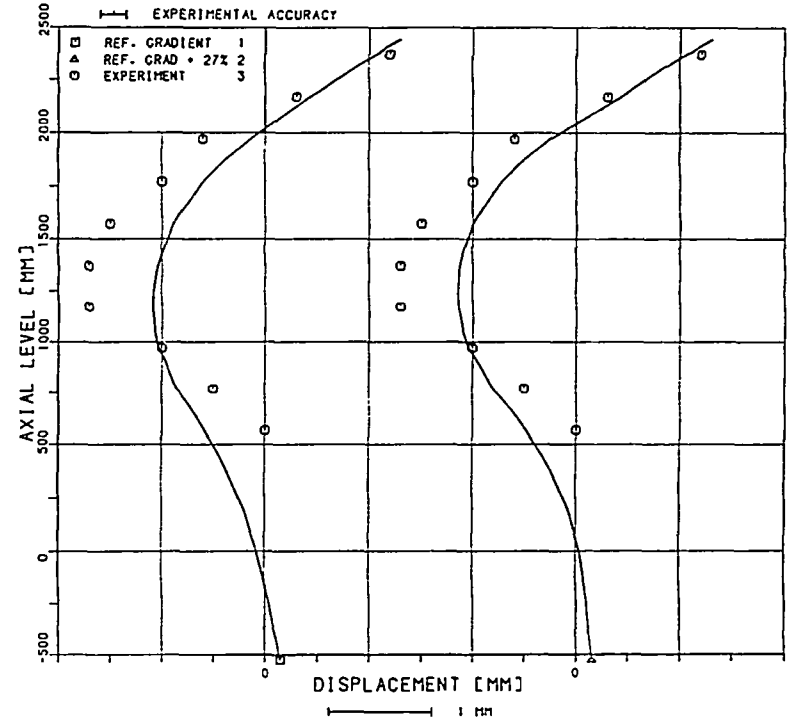

IWGFR STAGE 2 DDT EXAMPLE 1A
RESTRAINT BOW OF SINGLE S/A
LRP PAD STIFFNESS 2350 [N/MM]
VARIATION OF TEMP. GRADIENT

FIG. 2

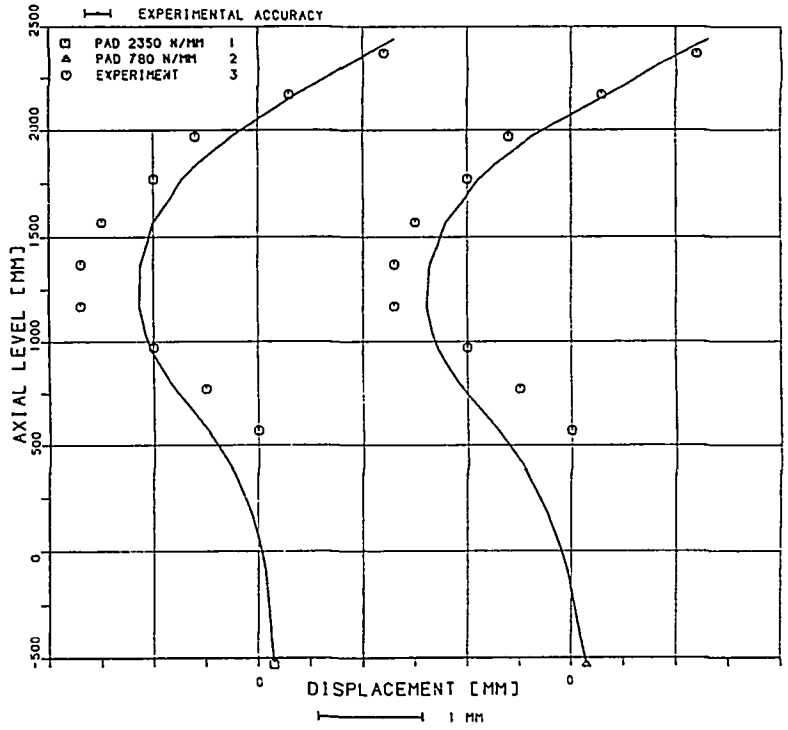

IWGFR STAGE 2 DDT EXAMPLE 1A
RESTRAINT BOW OF SINGLE S/A
REF. TEMP. GRADIENT + 27%
VARIATION OF LRP PAD STIFFNESS

FIG. 3

4.3 Example 2

- Restraint bow of a row of 10 subassemblies

Table 4 presents deflections resulting from the reference calculation for Example 2. A comparison with the measured values in Table 6 shows a good agreement for subassemblies No. 3 to 9 and a satisfactory agreement for subassemblies 0 to 2. This is also illustrated in Figure 4 which shows the bending lines of the 10 subassembiles. It has to be considered that in this figure the distances and gaps between the subassemblies are not according to scale.

Table 4: EXAMPLE 2

Restraint deflections [mm] of a row of 10 subassemblies.
DDT-reference calculation with a pad stiffness of 2350 N/mm in LRP.

Axial Position [mm]	S/A-Number									
	0	1	2	3	4	5	6	7	8	9
570	0.0	-0.10	-0.24	-0.36	-0.34	-0.56	-0.62	-0.73	-0.86	0.25
770	0.12	-0.10	-0.28	-0.41	-0.42	-0.71	-0.77	-0.99	-1.21	0.32
970	0.23	-0.02	-0.20	-0.34	-0.40	-0.74	-0.79	-1.15	-1.44	0.40
1170	0.31	0.17	0.03	-0.11	-0.24	-0.58	-0.65	-1.19	-1.52	0.49
1370	0.37	0.44	0.44	0.30	0.08	-0.25	-0.34	-1.09	-1.44	0.58
1570	0.39	0.80	1.06	0.89	0.57	0.24	0.16	-0.86	-1.21	0.67
1770	0.36	1.25	1.86	1.67	1.19	0.88	0.83	-0.49	-0.82	0.76
1970	0.27	1.80	2.80	2.65	1.92	1.67	1.66	0.02	-0.26	0.85
2170	0.14	2.43	3.83	3.77	2.72	2.57	2.58	0.62	0.44	0.94
2370	0.0	3.09	4.89	4.93	3.54	3.52	3.52	1.23	1.20	1.05

Table 5: EXAMPLE 2

Restraint deflections [mm] of a row of 10 subassemblies.
DDT-reference calculation with a pad stiffness of 4700 N/mm in LRP.

Axial Position [mm]	S/A-Number									
	0	1	2	3	4	5	6	7	8	9
570	-0.09	-0.18	-0.30	-0.39	-0.36	-0.56	-0.61	-0.70	-0.80	0.25
770	-0.01	-0.21	-0.35	-0.46	-0.45	-0.71	-0.76	-0.94	-1.12	0.32
970	0.07	-0.14	-0.29	-0.40	-0.43	-0.74	-0.78	-1.09	-1.33	0.40
1170	0.13	0.28	-0.07	-0.17	-0.26	-0.58	-0.64	-1.11	-1.40	0.49
1370	0.19	0.28	0.33	0.23	0.06	-0.25	-0.33	-1.02	-1.31	0.58
1570	0.22	0.62	0.93	0.81	0.55	0.24	0.17	-0.79	-1.10	0.67
1770	0.22	1.05	1.72	1.58	1.18	0.88	0.84	-0.43	-0.73	0.76
1970	0.17	1.59	2.64	2.55	1.91	1.67	1.66	0.06	-0.19	0.85
2170	0.09	2.20	3.66	3.67	2.71	2.57	2.58	0.64	0.48	0.94
2370	-0.01	2.84	4.70	4.82	3.54	3.52	3.52	1.23	1.20	1.05

Table 6: EXAMPLE 2

Restraint deflections [mm] of a row of 10 sub-assemblies.
Results of measurements.

Axial Position [mm]	S/A-Number									
	0	1	2	3	4	5	6	7	8	9
570	0.5	0	-0.5	0	-0.5	0	-0.5	-1.0	-0.75	0
770	0	-0.25	-0.5	-0.25	-0.5	-0.5	-0.75	-1.25	-1.0	0
970	0	0	-0.5	-0.25	-0.5	-0.5	-0.5	-1.0	-1.25	0
1170	0	0	-0.25	0	-0.25	-0.5	-0.5	-1.25	-1.50	0.25
1370	0	0	0	0.25	0	-0.25	0	-1.0	-1.25	0.50
1570	0	0.25	0.5	0.75	0.5	0	0.25	-0.75	-0.75	0.25
1770	0	1.0	1.5	1.25	1.0	1.0	0	-0.5	-0.5	0.50
1970	0	1.25	2.5	2.25	2.75	2.0	1.75	-0.25	-0.75	1.0
2170	0	2.0	3.5	3.25	3.5	3.0	3.5	1.0	0.5	0.75
2370	0	3.25	4.0	4.5	4.25	4.25	4.25	1.25	1.25	1.0

The agreement between measurement and calculation is less good for the loads expecially as the calculated lower support load for subassembly 0 is 0 instead of measured 147 N (Table 7).

Increasing the lower pad stiffness of all subassemblies to 4700 N/mm results in a little bit better agreement concerning the deflections (Table 5, 7 and Figure 5) but does not yet lead to a gap closure at the lower support.

Also an additional change of all temperature profiles by +27 % has only very small effects on the deflections and does not change the gap distribution. So there are no extra values presented here.

Further information about the calculation results is given in Figures 6 to 9 where the loads of all subassemblies in all contact levels are presented.

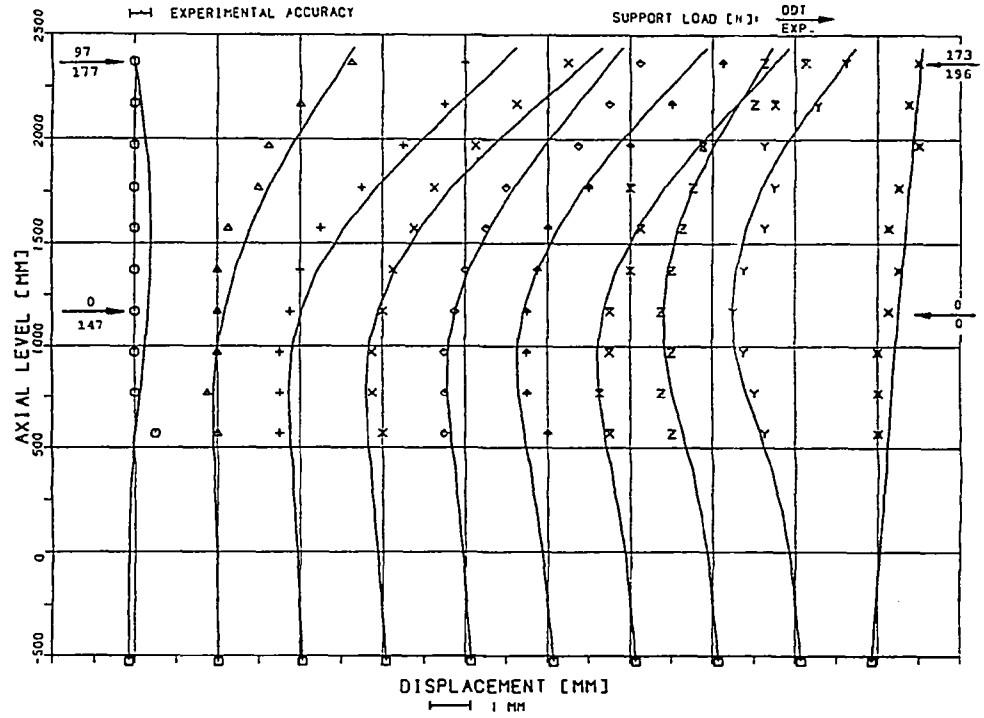

IWGFR BENCHMARK STAGE 2
DDT - RESULTS FOR EXAMPLE 2
RESTRAINT BOW OF 10 S/A
LRP PAD STIFFNES 2350 [N/MM]

FIG. 4

Table 7: EXAMPLE 2

Support loads [N] for experiment and DDT-calculations with different assumptions for pad-stiffness

Axial Position [mm]	Experiment		DDT-Reference 2350 N/mm		DDT-Variation 4700 N/mm	
	S/A		S/A		S/A	
	0	9	0	9	0	9
URP	177	196	97	173	123	199
LRP	147	0	0	0	0	0

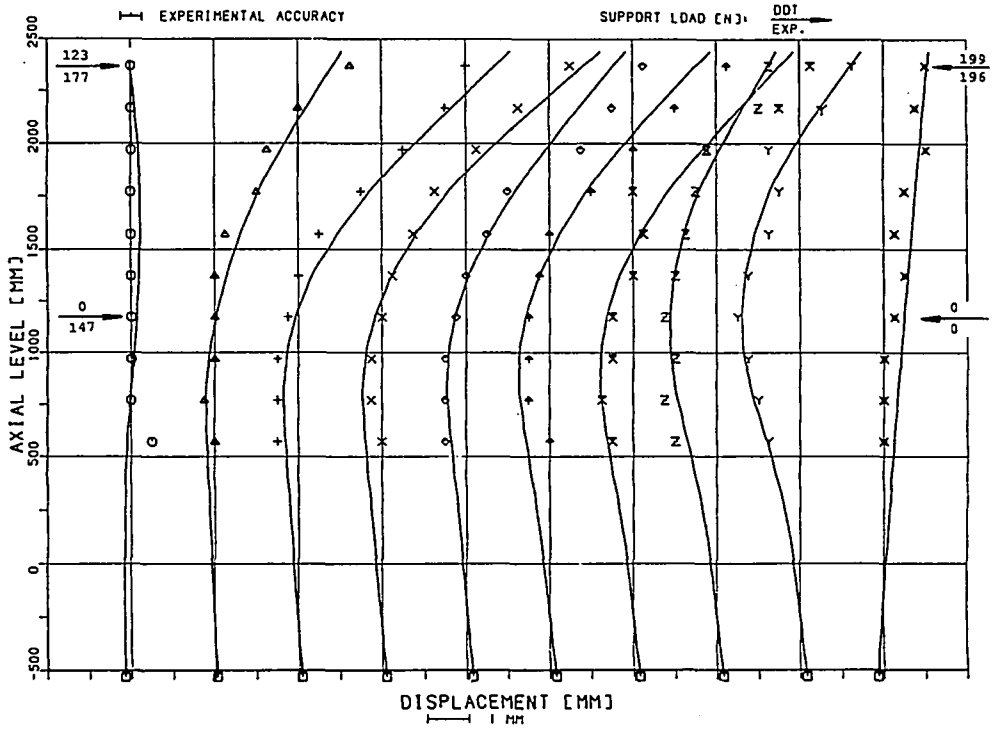

IWGFR BENCHMARK STAGE 2
DDT - RESULTS FOR EXAMPLE 2
RESTRAINT BOW OF 10 S/A
LRP PAD STIFFNESS 4700 [N/MM]

FIG. 5

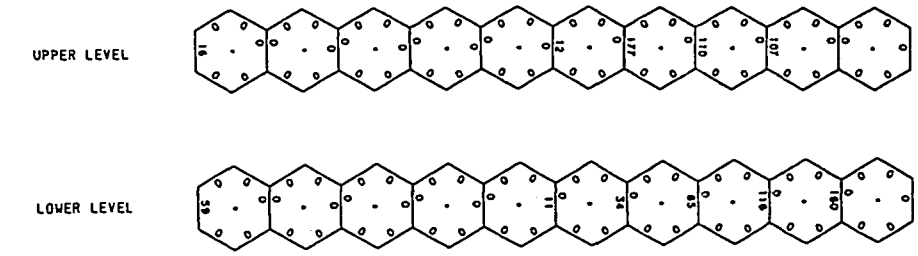

X 1 MM

FORCES IN SPIKE CONTACT LEVELS [N]

PAD STIFFNESS 2350 [N/MM] (REFERENCE)

IWGFR STAGE 2
EXAMPLE 2 DT=1.0
RESTRAINT BOW OF 10 S/A

FIG. 6

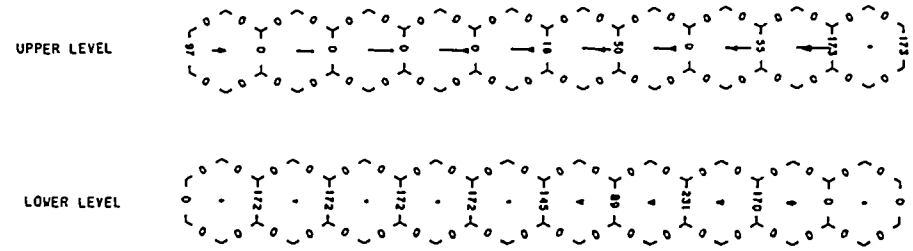

X 1 MM

FORCES IN SPACER PAD LEVELS [N]

PAD STIFFNESS 2350 [N/MM] (REFERENCE)

IWGFR STAGE 2
EXAMPLE 2 DT=1.0
RESTRAINT BOW OF 10 S/A

FIG. 7

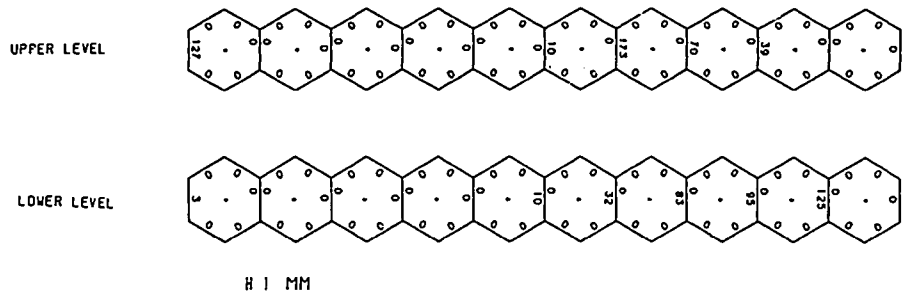

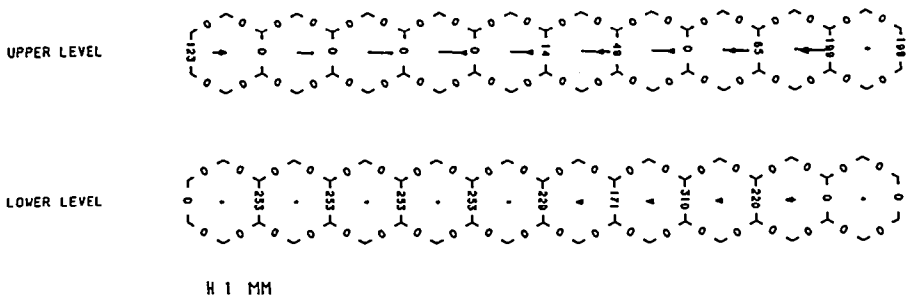

4.4 Example 3

- Single subassembly bending test

Figure 10 and Table 8 show results of 2 calculations with FIAT for the bending test of example 3.

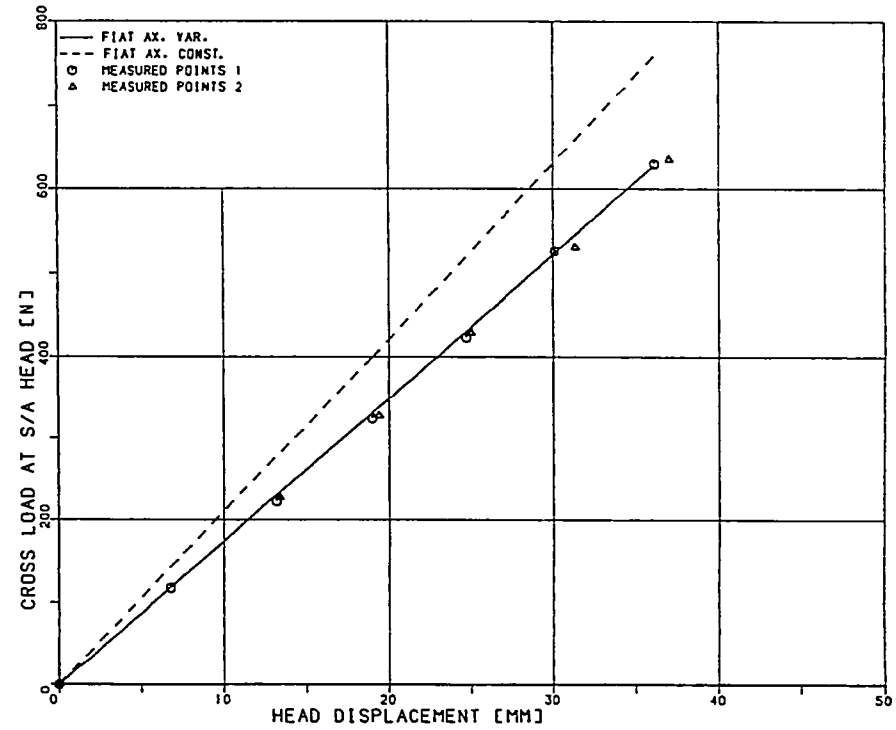

IWGFR BENCHMARK STAGE 2
FIAT - RESULTS FOR EXAMPLE 3
FORCED BOW OF A SINGLE S/A
FIG. 10

Table 8: EXAMPLE 3

Cross loads [N] and head displacements [mm] for experiments (Test 1 and Test 2) and FIAT-calculations

Displacement of S/A head [mm]	Cross load at S/A head [N]		
	FIAT; cross-sections are		Experiment Test 1 cross flats
	axial variable	axial constant	
6.8	118	143	117
13.2	230	278	222
19.0	331	399	324
24.7	430	519	423
30.1	524	633	526
36.1	628	759	630

Displacement of S/A head [mm]	Cross load at S/A head [N]		
	FIAT; cross-sections are		Experiment Test 2 cross corners
	axial variable	axial constant	
13.4	233	282	227
19.4	337	408	328
25.0	435	526	429
31.3	544	658	531
37.0	644	778	636

One calculation considers the spike geometry as axial variable, corresponding to the geometry in Figures 1 to 4 of Appendix 4 of the Enclosure. There is a good agreement between measured and calculated loads.

Another calculation considers the cross section geometry as axial constant, correspoonding to the geometry of the wrapper tube. The result is an overestimation of the loads of about 20 %. The same results would have been attained with DDT.

Figure 11 shows the axial dependence of the moment of inertia as calculated in FIAT for the given geometry. It can be seen that the vaule for the wrapper tube region is about 3 times larger than the value for the main part of the spike. A comparison with the geometry of the subassemblies of Examples 1 and 2 shows that in these cases the difference between the moments of inertia for spike and wrapper tube is smaller.

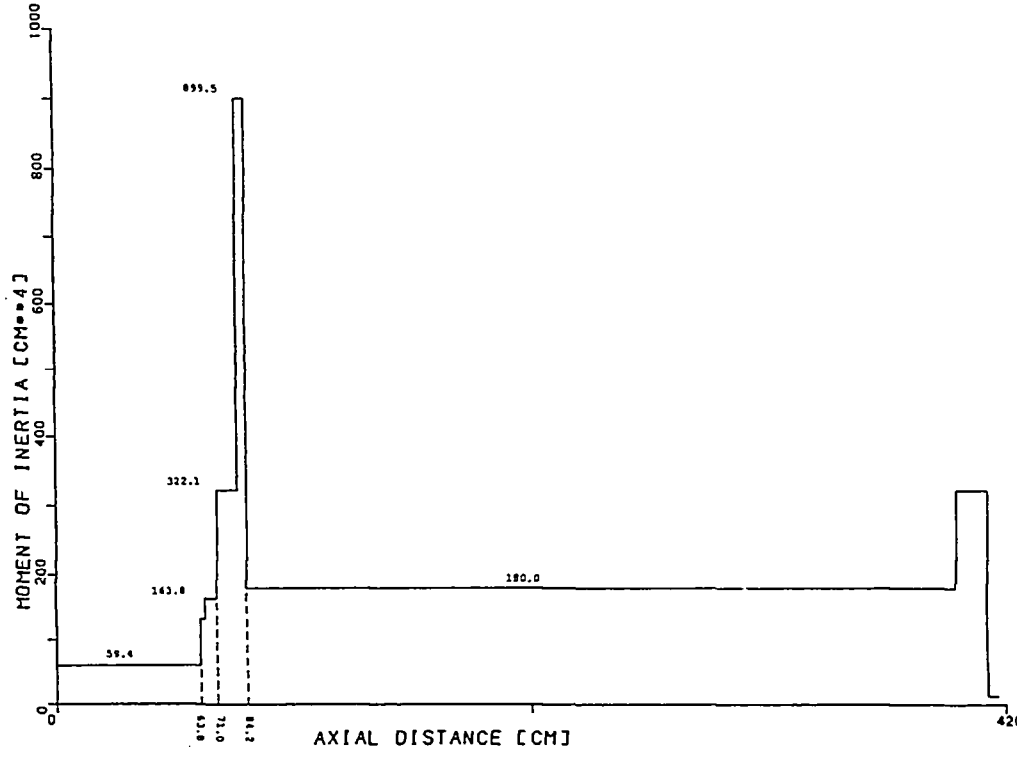

IWGFR BENCHMARK STAGE 2
FIAT - RESULTS FOR EXAMPLE 3
MOMENTS OF INERTIA

FIG. 11

REFERENCES

[1] V. Arkhipov
Consultants Meeting of the Co-ordinated Research Programme on Intercomparison of LMFBR Core Mechanics Codes
VIC, 8 - 10 December 1987
Summary Report from 25.03.1988

[2] R. Menssen
DDT - A 3-dimensinal Program for the Analysis of Bowed Reactor Cores
4th SMIRT, Vol. D, August 1977

[3] R. Menssen
Abschlußbericht des Forschungs- und Entwicklungsauftrages RS248
Erstellung und Überprüfung eines 3D-Programmes zur Bestimmung von Elementverbiegungen im Kernverband von Schnellen Brutreaktoren
Interatom-Report INTAT 33.01793.5, December 1979

[4] K. Urban
Analysis of Bower Reactor Cores Using the FIAT-Programme
4th SMIRT-Conference San Francisco 1977

[5] IAEA/IWGFR Coordinated Research Programme on Intercomparison of FMFBR Core Mechanics Codes - Japanese Ex-reactor Data for the Validation Exercise
Revised Edition PNC SN9450 88-003, April 1988

ENCLOSURE

THE JAPANESE EX-REACTOR DATA FOR THE VALIDATION EXERCISE

For reasons of space, this appendix is not included in this publication but may be found in Appendix 4 of the Final Report of the Co-ordinated Research Programme on Intercomparison of LMFBR Core Mechanics Codes entitled 'Verification and Validation of LMFBR Static Core Mechanics Codes, Part I', IWGFR/75, IAEA, Vienna (1990).